Nuclear Shadowing in Inelastic Photon-Nucleus Scattering in UPCs with Forward Neutrons

M. ALVIOLI [1,2], V. GUZEY [3], M. STRIKMAN [4]

[1] *Consiglio Nazionale delle Ricerche, Istituto di Ricerca per la Protezione Idrogeologica, via Madonna Alta 126, I-06128, Perugia, Italy*

[2] *Istituto Nazionale di Fisica Nucleare, Sezione di Perugia, via Pascoli 23c, I-06123, Perugia, Italy*

[3] *University of Jyvaskyla, Department of Physics, P.O. Box 35, FI-40014 University of Jyvaskyla, Finland and Helsinki Institute of Physics, P.O. Box 64, FI-00014 University of Helsinki, Finland*

[4] *Pennsylvania State University, University Park, PA, 16802, USA*

We argue that measurements of forward neutrons from nuclear breakup in inclusive high energy photon-nucleus (γA) scattering provide a novel complementary way to study small-x dynamics of QCD in heavy-ion ultraperipheral collisions (UPCs). Using the leading twist approach to nuclear shadowing, we calculate the distribution over the number of evaporation neutrons produced in γPb collisions at the LHC. We demonstrate that it allows one to determine the distribution over the number of wounded nucleons (inelastic collisions), which constrains the mechanism of nuclear shadowing of nuclear parton distributions and gives an access to their impact parameter dependence.

DOI: https://doi.org/10.17161/fnzwt563

Keywords: Heavy-ion scattering, ultraperipheral collisions, nuclear shadowing

1 Introduction

One of the main directions of modern high-energy nuclear physics is understanding of the dynamics of strong interactions and the structure of nuclei and nucleons in terms of quantum chromodynamics (QCD). Among many open questions, the limit of very high energies (small momentum fractions x) is of particular interest since it is predicted that the linear Dokshitzer-Gribov-Lipatov-Altarelli-Parisi (DGLAP) approximation for parton distributions (PDFs) will eventually break down [1,2] and a new, non-linear regime of high parton densities characterized by their saturation will set it [3,4]. Experimental studies of this and other open QCD questions are carried out at the Large Hadron Collider (LHC) [5,6] and the Relativistic Heavy Ion Collider (RHIC) and are planned at the future Electron-Ion Collider (EIC) at Brookhaven National Laboratory [7,8]. Note that heavy-ion scattering at the LHC and electron-nucleus collisions at the EIC present two complementary options for studying small-x QCD: while at the LHC practically all data are collected for the nucleus of lead (Pb), and the large collision energy and detector geometry allow one to probe down to $x \sim 10^{-5} - 10^{-4}$, the EIC will employ a wide array of light and heavy nuclei and will reach $x \sim 10^{-3}$ for momentum transfers of a few GeV.

An important part of the heavy-ion program at the LHC is related to ultraperipheral collisions (UPCs), where a photon emitted by one of the nuclei interacts with the other nucleus [9]. The focus of such measurements has so far been coherent and incoherent production of light and heavy vector mesons. In particular, over the last decade the data discovered a significant nuclear suppression of coherent J/ψ photoproduction in Pb-Pb UPCs compared to the impulse approximation prediction, see [10] for references. When interpreted in terms of the gluon distribution [11], it amounts to strong gluon nuclear shadowing [12,13], $R_{\rm Pb}^g(x,Q^2) = g_A(x,Q^2)/[Ag_N(x,Q^2)] \approx 0.6$ at $x = 10^{-3}$ and $R_{\rm Pb}^g(x,Q^2) \approx 0.5$ for $x = 10^{-5} - 10^{-4}$ at $Q^2 = 3$ GeV^2, where $g_A(x,Q^2)$ and $g_N(x,Q^2)$ are the nucleus and nucleon gluon densities, respectively. These values of $R_{\rm Pb}^g$ agree very well with the predictions of the leading twist approximation (LTA) for nuclear shadowing made more than 10 years ago [14]. The recent STAR data [15] indicate that the nuclear

©This work is an open access article under a Creative Commons Attribution 4.0 International License (https://creativecommons.org/licenses/by/4.0/).

suppression persists also for larger x, $R^g_{\rm Pb}(x,Q^2)=\sqrt{S^{\rm Au}_{\rm coh}}=0.84\pm0.05$ at $\langle x\rangle=0.015$.

Note that this interpretation of the J/ψ UPC data in terms of the gluon nuclear shadowing is complicated at the next-to-leading order (NLO) of the perturbative expansion in powers of $\log Q^2$ (perturbative QCD) by large cancellations between the leading-order (LO) and NLO gluon coefficient functions, which leaves a numerically important quark contribution [16,17]. A method to stabilize the perturbation series and restore the gluon dominance in this process on the proton target was suggested in [18,19].

Other hard UPC processes considered in the literature are inclusive [20,21] and diffractive [22,23] dijet photoproduction (there is preliminary ATLAS data for this process [24,25]), timelike Compton scattering [26,27,28], and heavy quark photoproduction [29,30,31].

In this contribution, we would like to outline several new directions of future UPC studies, which were not discussed in the review [9]. We explore for the first time the possibility to probe small-x nuclear shadowing by measuring the rates of forward neutron production from nuclear breakup in the zero degree calorimeters (ZDCs) at the LHC. Our numerical studies demonstrate that the number of produced neutrons is correlated with the number of wounded nucleons (inelastic photon-nucleon interactions), which presents a complementary way to study the mechanism of nuclear shadowing of nuclear PDFs. Importantly, it allows one to effectively access the centrality (impact parameter) dependence of nuclear PDFs.

This contribution is organized as follows. In Sec. 2 we summarize expectations based on applications of the Abramovski-Gribov-Kancheli (AGK) theorem to photon-nucleus scattering, model the distribution over the number of wounded nucleons and estimate its average value in the current UPC kinematics. Section 3 presents our predictions for the distributions over the number of emitted forward neutrons from nuclear breakup in inelastic photon-nucleus scattering and its connection to parameters of the leading twist approximation of nuclear shadowing. Our conclusions and outlook are given Sec. 4.

2 Abramovski-Gribov-Kancheli (AGK) cutting rules, nuclear shadowing and the number of wounded nucleons in γA scattering

It was demonstrated by Abramovski, Gribov and Kancheli in 1973 [32] that different unitary cuts of the diagrams corresponding to multi-Pomeron (color singlet) exchanges result in different multiplicities of produced particles in the central rapidity region and that the absorptive part of the amplitude can be expressed in terms of a small number of cut diagrams, which are related by combinatorial factors; these are the so-called Abramovski-Gribov-Kancheli (AGK) cutting rules or the AGK cancellation. For the interpretation of the AGK rules in QCD and other effective field theories, see Refs. [33,34,35,36,37].

In our analysis, we employ the following two applications of the AGK cutting rules to real photon-nucleus scattering. First, they allow one to express the nuclear shadowing correction to the total nuclear cross section $\sigma^{\gamma A}_{\rm tot}$ in terms of the diffractive cross section on individual nucleons. Further, using the QCD factorization theorem for hard diffraction [38], the connection between nuclear shadowing and diffraction can be established at the level of leading twist nuclear PDFs of individual flavors (quarks and gluons) [14,39].

Second, defining the total photon-nucleus inelastic cross section $\sigma^{\gamma A}_{\rm inel}$ as the difference between the total and total elastic (coherent plus incoherent) cross sections, it can be presented in the following form [40,41]

$$\sigma^{\gamma A}_{\rm inel}=\sum_{\nu=1}^{A}\sigma_\nu\,, \tag{1}$$

where

$$\sigma_\nu=\frac{A!}{(A-\nu)!\nu!}\int d^2\vec{b}\int d\sigma P_\gamma(\sigma)(\sigma_{\rm inel}T_A(\vec{b}))^\nu(1-\sigma_{\rm inel}T_A(\vec{b}))^{A-\nu}\,. \tag{2}$$

Equation (2) generalizes the expression for σ_ν in hadron-nucleus scattering to the case of photon-nucleus scattering, where the photon is represented by its hadronic fluctuations with the distribution $P_\gamma(\sigma)$. In Eq. (2), $\vec{b}$ is the impact parameter (transverse coordinate) of the interacting nucleon, $T_A(\vec{b})=\int dz\rho_A(\vec{b},z)$, where $\rho_A(\vec{b},z)$ is the nuclear density normalized to unity, and $\sigma_{\rm inel}=0.85\,\sigma$ is the inelastic cross section for the interaction of a hadronic fluctuation of the photon with a target nucleon, which is based on the estimate that the ρ meson-nucleon elastic cross section constitutes approximately 15% of the total one. The cross sections σ_ν are positive and represent the physical process, where ν nucleons undergo inelastic scattering, while the remaining $A-\nu$ nucleons provide absorption. In the literature, one uses the term "wounded nucleons" [42] and the notation $\nu=N_{\rm coll}$.

The distribution $P_\gamma(\sigma)$ gives the probability density for hadronic fluctuations of the real photon to interact with nucleons with the cross section σ [41,43]. The shape of $P_\gamma(\sigma)$ cannot be calculated from the

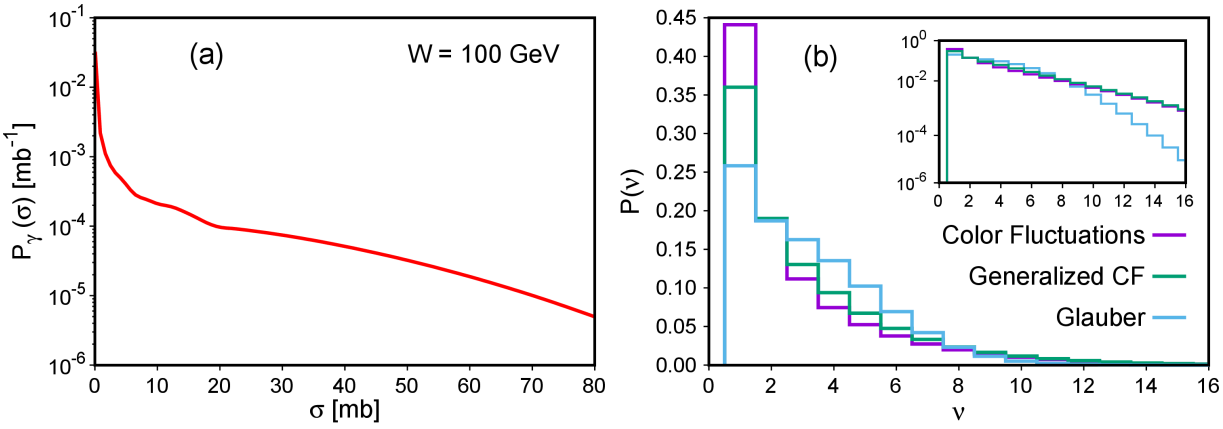

Figure 1 – (a) The distribution $P_\gamma(\sigma)$ as a function of σ at $W = 100$ GeV. (b) The distribution $P(\nu)$ for inelastic photon-nucleus (Pb) scattering as a function of the number of wounded nucleons ν. The three curves correspond to three models for $P_\gamma(\sigma)$, see text for details. The insert emphasizes the region of large ν.

first principles, but one can model it using its first moments and the small-σ and large-σ limits. Indeed, the total photon-proton cross section $\sigma_{\gamma p}(W)$ and the cross section of photon diffractive dissociation on the proton $d\sigma_{\gamma p\to Xp}(W, t=0)/dt$ constrain the first two moments of $P_\gamma(\sigma)$,

$$\begin{aligned} \sigma_{\gamma p}(W) &= \int d\sigma P_\gamma(\sigma)\sigma\,, \\ \frac{d\sigma_{\gamma p}(W,t=0)}{dt} &= \frac{1}{16\pi}\int d\sigma P_\gamma(\sigma)\sigma^2\,, \end{aligned} \tag{3}$$

where W is the invariant photon-nucleon center-of-mass-energy. Further, in the small-σ limit, one can express $P_\gamma(\sigma)$ in terms of the quark-antiquark component of the photon light-cone wave function and the color dipole cross section, which leads to $P_\gamma(\sigma) \propto 1/\sigma$. In the opposite limit of large σ, the photon behaves as a superposition of the ρ, ω and ϕ vector mesons in the spirit of the vector meson dominance model and, hence, $P_\gamma(\sigma)$ can be modeled using hadronic (cross section) fluctuations in ρ mesons, which in turn are related to those for pions. Finally, the small-σ and large-σ limits can be smoothly interpolated. Note that this matching is achieved best, when the light quark masses m_q are taken to be those of the constituent quarks, $m_q \sim 300$ MeV. For details, see [41,43].

The left panel of Fig. 1 presents the distribution $P_\gamma(\sigma)$ as a function of σ at $W = 100$ GeV. Since the W dependence of $P_\gamma(\sigma)$ is weak, the presented distribution is applicable in a wide range of energies probed in heavy-ion UPCs at the LHC. Note that the distribution $P_\gamma(\sigma)$ parametrizes the so-called resolved photon contribution to photon-induced scattering and does contain the direct photon contribution.

Using Eqs. (1) and (2), one can readily define the probability distribution over the number of wounded nucleons ν in inelastic photon-nucleus scattering, $P(\nu)$, as follows [41],

$$P(\nu) = \frac{\sigma_\nu}{\sum_{\nu=1}^{A}\sigma_\nu}\,, \tag{4}$$

where σ_ν are given by Eq. (2).

In our numerical analysis of Eq. (4), we use the Monte Carlo generator for nucleon configurations in complex nuclei [44], which also includes nucleon-nucleon correlations in the nucleus wave function [45,46]. The resulting distribution $P(\nu)$ as a function of ν for lead (^{208}Pb) is shown by the curve labeled "Color Fluctuations" in the right panel of Fig. 1.

The small-σ behavior of $P_\gamma(\sigma)$ is derived using the quark-antiquark component of the photon wave function, which does not capture the observed strong gluon nuclear shadowing discussed in Introduction. To take it into account, we model the nuclear suppression of the dipoles with $\sigma \le \sigma_0 = 20$ mb by the factor of R_A^g, which leads to the modified distribution $\tilde{P}_\gamma(\sigma)$,

$$\tilde{P}_\gamma(\sigma) = \left[R_A^g(x,Q^2)\theta(\sigma_0-\sigma) + \theta(\sigma-\sigma_0)\right] P_\gamma(\sigma)\,, \tag{5}$$

where $x = Q^2/W^2$ and $Q^2 = 3$ GeV^2. The distribution $P(\nu)$ corresponding to σ_ν, which is calculated using $\tilde{P}_\gamma(\sigma)$, is given by the curve "Generalized CF" in the right panel of Fig. 1.

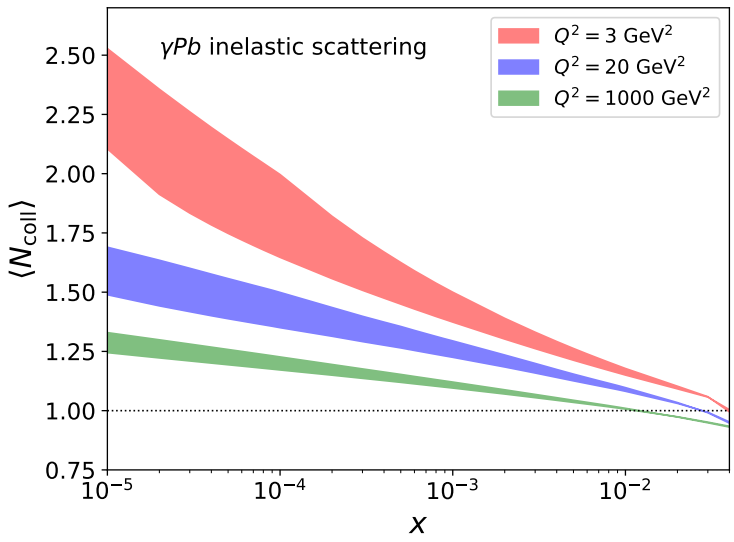

Figure 2 – The LTA predictions for the average number of wounded nucleons $\langle N_{\rm coll}\rangle$ in inelastic photon-nucleus (Pb) scattering as a function of x at $Q^2 = 3$, 20, and 1000 GeV^2.

Finally, to test the importance of cross section fluctuations in the real photon, we calculated $P(\nu)$ neglecting these fluctuations and using

$$P_\gamma(\sigma) = \delta(\sigma - 25\,{\rm mb})\,. \tag{6}$$

The result is given by the curve "Glauber" in Fig. 1. One can see from this figure that cross section (color) fluctuations in the real photon significantly increase the distribution $P(\nu)$ at small and large ν; the latter is emphasized in the insert.

In the total inelastic photon-nucleus cross section $\sigma_{\rm inel}^{\gamma A}$, the AGK cancellations manifest themselves as the observation that the average number of wounded nucleons $\langle N_{\rm coll}\rangle$ is inversely proportional to the nuclear shadowing factor. Generalizing the result of [40] for hadron-nucleus scattering to the case of photon-induced scattering, one obtains

$$\langle N_{\rm coll}\rangle \equiv \sum_{\nu=1}^{A} P(\nu)\nu = \frac{\sum_{\nu=1}^{A}\nu\sigma_\nu}{\sum_{\nu=1}^{A}\sigma_\nu} = \frac{A\sigma_{\rm inel}^{\gamma N}}{\sigma_{\rm inel}^{\gamma A}}\,, \tag{7}$$

where $\sigma_{\rm inel}^{\gamma N}$ is the photon-nucleon inelastic cross section. Considering a particular hard process in inelastic photon-nucleus scattering that probes the nuclear gluon distribution, e.g., inclusive charmonium (bottomonium) production $\gamma + A \to J/\psi(\Upsilon) + X$ or inclusive heavy-quark dijet production $\gamma + A \to Q\bar{Q} + X$, one obtains using Eq. (7),

$$\langle N_{\rm coll}\rangle \approx \frac{1}{R_{\rm Pb}^g(x,Q^2)} \lesssim 2\,. \tag{8}$$

In this estimate we used the numerical values for $R_{\rm Pb}^g(x,Q^2)$ discussed in Introduction and the observation that within LTA theoretical uncertainties, the effects of nuclear shadowing in the total and inelastic photon-nucleus cross sections are approximately equal.

Figure 2 shows LTA predictions for the average number of wounded nucleons $\langle N_{\rm coll}\rangle = 1/R_{\rm Pb}^g(x,Q^2)$ in inelastic photon-nucleus (Pb) scattering as a function of x at $Q^2 = 3$, 20, and 1000 GeV^2. These values of Q^2 correspond to photoproduction of J/ψ, Υ, and high-p_T dijets, respectively. One can see from the figure that in the discussed kinematics, the average number of wounded nucleons is modest and the series in Eq. (7) converges rather rapidly. In particular, we have checked that it is saturated by first six terms with a 5% precision. Note, however, that the convergence slows down in the limit of small x.

Measurements of $\langle N_{\rm coll}\rangle$ present a new method to study nuclear shadowing in inelastic photon-nucleus scattering. Unlike the observables used so far, the constraint of Eq. (8) indicates that one can perform a "Pomeron surgery" of nuclear shadowing by cutting a small number of Pomeron exchanges controlling the number of inelastic interactions with target nucleons. As a result, it gives an opportunity for an experimental determination of a small number of parameters quantifying nuclear shadowing, which leads to a systematic improvement of its theoretical description.

3 The distributions over the number of wounded nucleons and forward neutrons from nuclear breakup

While the average number of inelastic interactions $\langle N_{\rm coll}\rangle$ encodes information on the energy and scale dependence of nuclear shadowing, its dependence on the impact parameter of the collision is averaged over. To obtain a more microscopic description of nuclear shadowing and access the impact parameter dependence of nuclear PDFs, one needs to determine not only $\langle N_{\rm coll}\rangle$, but also the entire distribution over the number of wounded nucleons. This can be done using experimental data on the neutron emission resulting from nucleus fragmentation in a given UPC process, e.g., in inclusive quarkonium or dijet photoproduction in heavy-ion UPCs with an additional condition of Xn neutrons in the zero degree calorimeter (ZDC) on the nuclear target side [24,25].

Experimental information on neutron emission in high energy scattering off heavy nuclei is sparse and comes essentially from the following two sources. The ALICE collaboration measured the distribution over $\langle N_{\rm coll}\rangle$ in proton-nucleus scattering, where it was determined by the energy release (E_T) at central rapidities [47]. It was observed that $\langle N_{\rm coll}(E_T)\rangle$ is linearly proportional to the number of evaporation neutrons $\langle M_n(E_T)\rangle$ for the same E_T bins at least up to $\langle N_{\rm coll}\rangle \sim 10$. Note that in our case, $\langle N_{\rm coll}\rangle$ is much lower, see Eq. (8).

Another important observation is the E665 experiment at Fermilab on muon-nucleus deep inelastic scattering (DIS) in coincidence with detection of slow neutrons, $\mu^- + A \to n + X$, which showed that the average neutron multiplicity $\langle M_n\rangle$ for the lead target is [48]

$$\langle M_n\rangle \approx 5\,. \tag{9}$$

This result has been understood in the framework of cascade models of nuclear DIS [49,50], where soft neutrons are produced either directly in DIS on a bound nucleon or through statistical decay (de-excitation) of the excited residual nucleus, leading to neutron evaporation. A similar conclusion was reached using the BeAGLE Monte Carlo generator [51].

It suggests the following space-time picture of forward neutron production in high energy photon-nucleus scattering. The incoming photon fluctuates into hadronic components, which pass through the nucleus and interact inelastically with several nucleons. This leads to the creation of holes in the nucleus (particle-hole excitations in terminology of a nuclear shell model), which de-excite and cool the nucleus by evaporating neutrons. It also produces a number of soft particles with the momenta less than 1 GeV/c, which in turn generate more neutrons.

The nucleon fragmentation weakly depends on the incident energy due to Feynman scaling and, hence, the energy transfer used to heat the residual nuclear system is proportional to $\langle N_{\rm coll}\rangle$. Since the Fermilab data [48] corresponds to the average momentum fraction $\langle x\rangle = 0.015$, where the nuclear shadowing effect is small, one finds that $\langle N_{\rm coll}\rangle \approx 1$, see Eq. (7). Thus, every inelastic photon-nucleon interaction results on average in 5 forward neutrons.

To test this hypothesis, we perform two numerical studies. First, we consider a simple model, which assumes that the probability density of neutron emission is given by the Poisson distribution and that each hole created in the target nucleus generates independently on average $\langle M_n\rangle$ neutrons. Therefore, the neutron probability distribution for $\nu = \langle N_{\rm coll}\rangle$ wounded nucleons is

$$P_{\rm Poisson}(N;\lambda=\nu\langle M_n\rangle) = \frac{(\nu\langle M_n\rangle)^N e^{-\nu\langle M_n\rangle}}{N!}\,, \tag{10}$$

where N is the number of produced neutrons (neutron multiplicity).

The resulting probability density (frequency) for ^{208}Pb as a function of N is shown in the left panel of Fig. 3. In this estimate, we used $\langle M_n\rangle = 5$, see Eq. (9), and $\nu = \langle N_{\rm coll}\rangle = 1, 2, 3$ independent neutron emissions. One can see from the figure that since the distributions for different ν are peaked at different values of N and do not significantly overlap, the measurement of the forward neutron multiplicity can be used to reliably separate contributions of different $\langle N_{\rm coll}\rangle$. Our analysis also shows that this separation becomes even cleaner with an increase of $\langle M_n\rangle$ (not shown here).

In the second study, we combine the distribution over the number of wounded nucleons $P(\nu)$ that we discussed in Sec. 2 with the Poisson distribution of produced neutrons. The resulting probability distribution of forward neutrons is given by the following convolution,

$$P_{\rm comb}(N) = \sum_{\nu=1}^{A} P(\nu) P_{\rm Poisson}(N;\nu\langle M_n\rangle)\,. \tag{11}$$

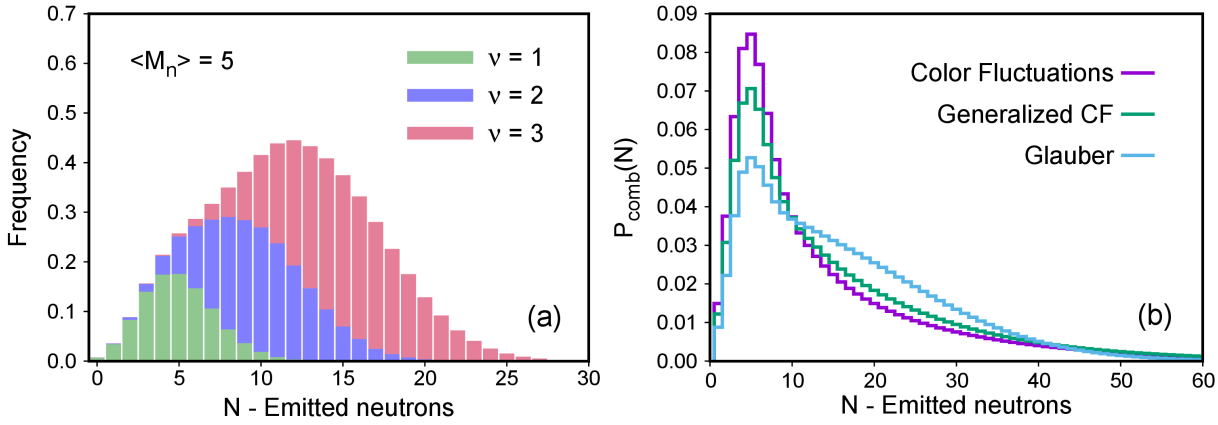

Figure 3 – (a) The probability distribution (frequency) for ^{208}Pb to produce N forward neutrons assuming their Poisson distribution with $\nu = \langle N_{\rm coll}\rangle = 1, 2, 3$ independent emissions and the average multiplicity for a single inelastic scattering $\langle M_n\rangle = 5$. (b) The probability distribution of forward neutron emission $P_{\rm comb}(N)$ (11) in the model combining the distribution over the number of wounded nucleons, which is calculated using three models for hadronic fluctuations in the photon (see Fig. 1), with the Poisson distribution of produced neutrons.

The right panel of Fig. 3 presents $P_{\rm comb}(N)$ as a function of forward neutrons N for $\langle M_n\rangle = 5$. The three curves correspond to the three models for $P_\gamma(\sigma)$, see the right panel of Fig. 1. One can see from the figure that cross section fluctuations in the real photon noticeably affect the shape of the neutron distribution: its maximum around $N = 5 - 7$ becomes higher and narrower compared to the "Glauber" result and is also somewhat suppressed by the leading twist shadowing in the "Generalized CF" case.

Our numerical studies suggest that one can examine details of the theoretical description of small-x nuclear shadowing in QCD using the distribution of forward neutrons from nuclear breakup emitted in a given hard UPC process, which is directly correlated with the number of inelastic interactions (wounded nucleons). By studying the dispersion of this distribution, one can single out the individual contributions of $\nu = 1, 2, 3, \ldots$ wounded nucleons. In particular, using Eq. (2) in the approximation that the series in Eq. (7) is saturated by first few terms, which corresponds to the limit of small-to-modest nuclear shadowing, one obtains [41,52]

$$\sigma_2(x,Q^2) \equiv \frac{\langle\sigma^2_{\rm inel}\rangle}{\langle\sigma_{\rm inel}\rangle} = \frac{\langle N_{\rm coll}-1\rangle}{\frac{(A-1)}{2}\int d^2\vec{b}\,T_A^2(\vec{b})}\,, \tag{12}$$

and

$$\sigma_3(x,Q^2) \equiv \frac{\langle\sigma^3_{\rm inel}\rangle}{\langle\sigma^2_{\rm inel}\rangle} = \frac{\langle\sigma^3_{\rm inel}\rangle}{\langle\sigma_{\rm inel}\rangle}\frac{\langle\sigma^2_{\rm inel}\rangle}{\langle\sigma^2_{\rm inel}\rangle} = \frac{(\langle N_{\rm coll}-2\rangle)(\langle N_{\rm coll}-1\rangle)}{\langle N_{\rm coll}-1\rangle}\frac{\frac{(A-1)}{2}\int d^2\vec{b}\,T_A^2(\vec{b})}{\frac{(A-2)(A-1)}{2}\int d^2\vec{b}\,T_A^3(\vec{b})}\,, \tag{13}$$

where $\langle\sigma^n_{\rm inel}\rangle = \int d\sigma P_\gamma(\sigma)\sigma^n_{\rm inel}$. The cross sections $\sigma_2(x,Q^2)$ and $\sigma_3(x,Q^2)$ are essential ingredients of the LTA approach [14]. While $\sigma_2(x,Q^2)$ is determined using the HERA data on inclusive diffraction in lepton-proton DIS, $\sigma_3(x,Q^2)$ is model-dependent and its variation leads to LTA theoretical uncertainties. Thus, an independent determination $\sigma_2(x,Q^2)$ and $\sigma_3(x,Q^2)$ using UPCs with forward neutrons will supply new constraints on these quantities.

Note that to reach a high accuracy in such an analysis, one needs to calibrate the theoretical description against the kinematics, where only one target nucleon is struck in $\gamma + A \to 2$ jets $+ X$ or quasi-elastic J/ψ production for $x_A \geq 0.01$, where the effect of nuclear shadowing is small and $\langle N_{\rm coll}\rangle \approx 1$.

4 Conclusions and outlook

In this contribution, we advertise measurements of forward neutrons from nuclear breakup in inclusive high energy photon-nucleus scattering in heavy-ion UPCs, e.g., charmonium (bottomonium) production $\gamma + A \to J/\psi(\Upsilon) + X$ or heavy-quark dijet production $\gamma + A \to Q\bar{Q} + X$, as a novel way to study the QCD dynamics at small x. The key quantity is the number of inelastic photon-nucleon interactions (the number of wounded nucleons): its average value $\langle N_{\rm coll}\rangle$ is proportional to inverse of the gluon nuclear shadowing factor and its first moments are sensitive to details of the leading twist mechanism of nuclear shadowing.

Our numerical analysis has demonstrated that the number of forward neutrons from nuclear breakup detected in the ZDC on the nuclear target side is rather unambiguously proportional to the number of wounded nucleons, which provides a practical opportunity for novel studies of nuclear shadowing.

On top of providing stringent tests of the dynamics of leading twist shadowing of gluon PDFs, it would be possible to explore effects related to proximity to the black disk limit of the strong interaction. For example, one can study fragmentation of leading hadrons in γA scattering and look for suppression of their multiplicity as a function of Feynman x_F and W as well as for broadening of their transverse momentum distribution [53]. These effects should be more pronounced for central collisions characterized by an enhanced activity in the ZDC. It should be possible to construct from the data an analog of the R_{CP} ratio, which would probe the density dependence of fragmentation. It would also be useful to construct similar quantities for low p_T charm production.

Another interesting application is for multiparton interactions in proton-nucleus (pA) scattering. It was argued in [54] that the single and double scattering can be separated using their dependence on the impact parameter: the former is proportional to A, while the latter $\propto A^{4/3}$. However, since both hard interactions are typically detected in a limited range of rapidities $|y| \leq 3-4$, centrality is difficult to determine from the transverse energy E_T signal because multiparton interactions also contribute to E_T. The use of forward neutrons in ZDCs would alleviate this problem.

One should point out that the neutrons detected in ZDCs can be a promising complementary way to determine centrality of various photon-nucleus and proton-nucleus inelastic collisions expanding the use of ZDCs beyond their current use in vector meson diffractive production and for determining of centrality of the heavy-ion collisions. The main advantage of using forward neutrons rather than the transverse energy E_T for the determination of centrality is a much larger distance in rapidity between the rapidity of the hard process and that of the process used for determination of the centrality.

One of the principal problems of using UPCs for studies of small-x phenomena is a lack of the nucleon reference data at similar energies with the precision necessary to observe nuclear effects with a better than 10% accuracy (J/ψ exclusive photoproduction is a notable exception). Here we outline a possible strategy for overcoming this problem. Note that we are not aiming to optimize cuts or to account for the energy resolution of ZDCs since this would require a dedicated Monte Carlo study.

One can separate events into two classes: peripheral events corresponding to $\langle N_{\rm coll}\rangle \leq 2$ (we call it class "L") and more central events corresponding to $\langle N_{\rm coll}\rangle \geq 1.5-2$ and $\langle M_n\rangle \sim 7-10$ (class "H"). If statistics is sufficient, the lower limit for class "H" can be gradually increased, which will push up the average number of wounded nucleons. Then, the ratio of the number of events in the two classes, $\hat{R} =$ Yield(H)/Yield(L), should quantify the effect of nuclear shadowing at small and large impact parameters, which in principle probes the dependence of nuclear shadowing on the thickness of nuclear matter. The promising channels for such an analysis include inclusive charm production with the transverse momentum in the range $p_T = 5-20$ GeV/c and production of soft particles with small $p_T < 0.5$ GeV/c. A comparison of the rates of these processes will allow one to study the transition between the soft and hard regimes and will serve as a consistency check of the description of small-x dynamics in the current models.

The methods presented in this paper can be readily generalized to the case of virtual photons and allow one to predict the distribution over the number of forward neutrons in inelastic (virtual) photon-nucleus scattering at the EIC.

Acknowledgments

The research of V.G. was funded by the Academy of Finland project 330448, the Center of Excellence in Quark Matter of the Academy of Finland (projects 346325 and 346326), and the European Research Council project ERC-2018-ADG-835105 YoctoLHC. The research of M.S. was supported by the US Department of Energy Office of Science, Office of Nuclear Physics under Award No. DE- FG02-93ER40771.

References

1. Y. L. Dokshitzer, D. Diakonov and S. I. Troian, Phys. Rept. **58**, 269-395 (1980)
2. L. V. Gribov, E. M. Levin and M. G. Ryskin, Phys. Rept. **100**, 1-150 (1983)
3. F. Gelis, E. Iancu, J. Jalilian-Marian and R. Venugopalan, Ann. Rev. Nucl. Part. Sci. **60**, 463-489 (2010) [arXiv:1002.0333 [hep-ph]].
4. A. Morreale and F. Salazar, Universe **7**, no.8, 312 (2021) [arXiv:2108.08254 [hep-ph]].
5. C. A. Salgado, J. Alvarez-Muniz, F. Arleo, N. Armesto, M. Botje, M. Cacciari, J. Campbell,

C. Carli, B. Cole and D. D'Enterria, *et al.* J. Phys. G **39**, 015010 (2012) [arXiv:1105.3919 [hep-ph]].
6. Z. Citron, A. Dainese, J. F. Grosse-Oetringhaus, J. M. Jowett, Y. J. Lee, U. A. Wiedemann, M. Winn, A. Andronic, F. Bellini and E. Bruna, *et al.* CERN Yellow Rep. Monogr. **7**, 1159-1410 (2019) [arXiv:1812.06772 [hep-ph]].
7. A. Accardi, J. L. Albacete, M. Anselmino, N. Armesto, E. C. Aschenauer, A. Bacchetta, D. Boer, W. K. Brooks, T. Burton and N. B. Chang, *et al.* Eur. Phys. J. A **52**, no.9, 268 (2016) [arXiv:1212.1701 [nucl-ex]].
8. R. Abdul Khalek, A. Accardi, J. Adam, D. Adamiak, W. Akers, M. Albaladejo, A. Al-bataineh, M. G. Alexeev, F. Ameli and P. Antonioli, *et al.* Nucl. Phys. A **1026**, 122447 (2022) [arXiv:2103.05419 [physics.ins-det]].
9. A. J. Baltz, G. Baur, D. d'Enterria, L. Frankfurt, F. Gelis, V. Guzey, K. Hencken, Y. Kharlov, M. Klasen and S. R. Klein, *et al.* Phys. Rept. **458**, 1-171 (2008)
10. M. Alvioli, V. Guzey and M. Strikman, [arXiv:2402.19060 [hep-ph]].
11. M. G. Ryskin, Z. Phys. C **57**, 89-92 (1993)
12. V. Guzey, E. Kryshen, M. Strikman and M. Zhalov, Phys. Lett. B **726**, 290-295 (2013) [arXiv:1305.1724 [hep-ph]].
13. V. Guzey and M. Zhalov, JHEP **10**, 207 (2013) [arXiv:1307.4526 [hep-ph]].
14. L. Frankfurt, V. Guzey and M. Strikman, Phys. Rept. **512**, 255-393 (2012) [arXiv:1106.2091 [hep-ph]].
15. [STAR], [arXiv:2311.13632 [nucl-ex]].
16. K. J. Eskola, C. A. Flett, V. Guzey, T. Löytäinen and H. Paukkunen, Phys. Rev. C **106**, no.3, 035202 (2022) [arXiv:2203.11613 [hep-ph]].
17. K. J. Eskola, C. A. Flett, V. Guzey, T. Löytäinen and H. Paukkunen, Phys. Rev. C **107**, no.4, 044912 (2023) [arXiv:2210.16048 [hep-ph]].
18. S. P. Jones, A. D. Martin, M. G. Ryskin and T. Teubner, J. Phys. G **43**, no.3, 035002 (2016) [arXiv:1507.06942 [hep-ph]].
19. S. P. Jones, A. D. Martin, M. G. Ryskin and T. Teubner, Eur. Phys. J. C **76**, no.11, 633 (2016) [arXiv:1610.02272 [hep-ph]].
20. M. Strikman, R. Vogt and S. N. White, Phys. Rev. Lett. **96**, 082001 (2006) [arXiv:hep-ph/0508296 [hep-ph]].
21. V. Guzey and M. Klasen, Phys. Rev. C **99**, no.6, 065202 (2019) [arXiv:1811.10236 [hep-ph]].
22. V. Guzey and M. Klasen, JHEP **04**, 158 (2016) [arXiv:1603.06055 [hep-ph]].
23. I. Helenius, SciPost Phys. Proc. **8**, 145 (2022) [arXiv:2107.07389 [hep-ph]].
24. [ATLAS], "Photo-nuclear dijet production in ultra-peripheral Pb+Pb collisions," ATLAS-CONF-2017-011.
25. [ATLAS], "Photo-nuclear jet production in ultra-peripheral Pb+Pb collisions at $\sqrt{s}_{\mathrm{NN}} = 5.02$ TeV with the ATLAS detector," ATLAS-CONF-2022-021.
26. B. Pire, L. Szymanowski and J. Wagner, Phys. Rev. D **79**, 014010 (2009) [arXiv:0811.0321 [hep-ph]].
27. W. Schafer, G. Slipek and A. Szczurek, Phys. Lett. B **688**, 185-191 (2010) [arXiv:1003.0610 [hep-ph]].
28. G. M. Peccini, L. S. Moriggi and M. V. T. Machado, Phys. Rev. D **103**, no.5, 054009 (2021) [arXiv:2101.08338 [hep-ph]].
29. S. R. Klein, J. Nystrand and R. Vogt, Phys. Rev. C **66**, 044906 (2002) [arXiv:hep-ph/0206220 [hep-ph]].
30. V. P. Goncalves, M. V. T. Machado and A. R. Meneses, Phys. Rev. D **80**, 034021 (2009) [arXiv:0905.2067 [hep-ph]].
31. V. P. Gonçalves, G. Sampaio dos Santos and C. R. Sena, Nucl. Phys. A **976**, 33-45 (2018) [arXiv:1711.04497 [hep-ph]].
32. V. A. Abramovsky, V. N. Gribov and O. V. Kancheli, Yad. Fiz. **18**, 595-616 (1973), Sov. J. Nucl. Phys. 18, 308-317 (1974).
33. D. Treleani, Int. J. Mod. Phys. A **11**, 613-654 (1996)
34. J. Jalilian-Marian and Y. V. Kovchegov, Phys. Rev. D **70**, 114017 (2004) [erratum: Phys. Rev. D **71**, 079901 (2005)] [arXiv:hep-ph/0405266 [hep-ph]].
35. F. Gelis and R. Venugopalan, Nucl. Phys. A **776**, 135-171 (2006) [arXiv:hep-ph/0601209 [hep-ph]].
36. A. Kovner and M. Lublinsky, JHEP **11**, 083 (2006) [arXiv:hep-ph/0609227 [hep-ph]].
37. N. N. Nikolaev and W. Schafer, Phys. Rev. D **74**, 074021 (2006) [arXiv:hep-ph/0607307 [hep-ph]].

38. J. C. Collins, Phys. Rev. D **57**, 3051-3056 (1998) [erratum: Phys. Rev. D **61**, 019902 (2000)] [arXiv:hep-ph/9709499 [hep-ph]].
39. L. Frankfurt and M. Strikman, Eur. Phys. J. A **5**, 293-306 (1999) [arXiv:hep-ph/9812322 [hep-ph]].
40. L. Bertocchi and D. Treleani, J. Phys. G **3**, 147 (1977)
41. M. Alvioli, L. Frankfurt, V. Guzey, M. Strikman and M. Zhalov, Phys. Lett. B **767**, 450-457 (2017) [arXiv:1605.06606 [hep-ph]].
42. A. Bialas, M. Bleszynski and W. Czyz, Nucl. Phys. B **111**, 461-476 (1976)
43. L. Frankfurt, V. Guzey, A. Stasto and M. Strikman, Rept. Prog. Phys. **85**, no.12, 126301 (2022) [arXiv:2203.12289 [hep-ph]].
44. M. Alvioli, H. J. Drescher and M. Strikman, Phys. Lett. B **680**, 225-230 (2009) [arXiv:0905.2670 [nucl-th]].
45. M. Alvioli, C. Ciofi degli Atti, I. Marchino, V. Palli and H. Morita, Phys. Rev. C **78**, 031601 (2008) [arXiv:0807.0873 [nucl-th]].
46. M. Alvioli, C. Ciofi degli Atti and H. Morita, Phys. Rev. Lett. **100**, 162503 (2008)
47. S. Acharya *et al.* [ALICE], JHEP **08**, 086 (2022) [arXiv:2107.10757 [nucl-ex]].
48. M. R. Adams *et al.* [E665], Phys. Rev. Lett. **74**, 5198-5201 (1995) [erratum: Phys. Rev. Lett. **80**, 2020-2021 (1998)]
49. M. Strikman, M. G. Tverskoii and M. B. Zhalov, Phys. Lett. B **459**, 37-42 (1999) [arXiv:nucl-th/9806099 [nucl-th]].
50. A. B. Larionov and M. Strikman, Phys. Rev. C **101**, no.1, 014617 (2020) [arXiv:1812.08231 [hep-ph]].
51. W. Chang, E. C. Aschenauer, M. D. Baker, A. Jentsch, J. H. Lee, Z. Tu, Z. Yin and L. Zheng, Phys. Rev. D **106**, no.1, 012007 (2022) [arXiv:2204.11998 [physics.comp-ph]].
52. M. Alvioli, L. Frankfurt, V. Guzey and M. Strikman, Phys. Rev. C **90**, 034914 (2014) [arXiv:1402.2868 [hep-ph]].
53. L. Frankfurt, V. Guzey, M. McDermott and M. Strikman, Phys. Rev. Lett. **87**, 192301 (2001) [arXiv:hep-ph/0104154 [hep-ph]].
54. M. Alvioli, M. Azarkin, B. Blok and M. Strikman, Eur. Phys. J. C **79**, no.6, 482 (2019) [arXiv:1901.11266 [hep-ph]].